

# Fermi National Accelerator Laboratory

FERMILAB-Pub-78/24-EXP  
7420.180

(Submitted to Phys. Rev. Lett.)

## DIFFRACTIVE PRODUCTION OF VECTOR MESONS IN HIGH ENERGY NEUTRINO INTERACTIONS

J. Bell, J. P. Berge, D. V. Bogert, R. J. Cence,  
C. T. Coffin, R. N. Diamond, F. A. DiBianca,  
R. Endorf, H. T. French, R. Hanft, F. A. Harris,  
M. Jones, C. Kochowski, W. C. Louis, G. R. Lynch,  
J. A. Malko, J. P. Marriner, G. I. Moffatt, F. A. Nezrick,  
S. I. Parker, M. W. Peters, V. Z. Peterson, B. P. Roe,  
R. T. Ross, W. G. Scott, A. A. Seidl, W. Smart,  
V. J. Stenger, M. L. Stevenson,  
J. C. Vander Velde, and E. Wang

Fermi National Accelerator Laboratory, Batavia, Illinois 60510  
Lawrence Berkeley Laboratory, Berkeley, California 94720  
University of Hawaii at Manoa, Honolulu, Hawaii 96822  
University of Michigan, Ann Arbor, Michigan 48109

February 1978

Diffraction Production of Vector Mesons  
in High Energy Neutrino Interactions\*

J. Bell, J.P. Berge, D.V. Bogert, R.J. Cence, C.T. Coffin, R.N. Diamond, F.A. DiBianca, R. Endorf, H.T. French, R. Hanft, F.A. Harris, M. Jones, C. Kochowski, W.C. Louis, G.R. Lynch, J.A. Malko, J.P. Marriner, G.I. Moffatt, F.A. Nezzrick, S.I. Parker, M.W. Peters, V.Z. Peterson, B.P. Roe, R.T. Ross, W.G. Scott, A.A. Seidl, W. Smart, V.J. Stenger, M.L. Stevenson, J.C. Vander Velde, E. Wang.

Fermi National Accelerator Laboratory, Batavia, IL. 60510 and Lawrence Berkeley Laboratory, Berkeley, CA. 94720 and University of Hawaii at Manoa, Honolulu, HI. 96822, and University of Michigan, Ann Arbor, MI. 48109.

ABSTRACT

Results for diffractive production of vector mesons in high energy neutrino proton interactions are presented. Diffractive production of  $\rho^+$  is observed with a cross section of  $8 \pm 3 \times 10^{-40} \text{ cm}^2$  in agreement with recent theoretical predictions. Upper limits for  $A_1^+$  and  $B^+$  production are presented. The limit for  $B^+$  production gives a new limit on the contribution of weak second-class currents.

\*Work supported in part by U.S. Department of Energy.

Diffraction production of vector mesons provides a direct test of the relation between weak and electro-magnetic currents hence their presence or absence has important consequences. Recent calculations have predicted rates for these processes<sup>(1)</sup>. We have searched for vector meson production in the reactions:

$$\text{Charged Current (CC): } \nu p \rightarrow \pi^+ \pi^+ \pi^- p \mu^- \quad (1)$$

$$\nu p \rightarrow \pi^+ \pi^0 p \mu^- \quad (2)$$

$$\nu p \rightarrow \pi^+ \pi^+ \pi^- \pi^0 p \mu^- \quad (3)$$

$$\text{Neutral Current (NC): } \nu p \rightarrow \pi^+ \pi^- p \nu \quad (4)$$

$$\nu p \rightarrow K^+ K^- p \nu \quad (5)$$

The data come from two exposures of the Fermilab 15 ft. bubble chamber, filled with hydrogen. The first (second) exposure of 70,000 (80,000) pictures was taken with a wide-band single-horn (two horn) focussed neutrino beam with primary proton energy of 300 GeV (400 GeV). With the higher beam intensity, the second exposure corresponds to ~ 75% of the data. The neutrino event energy spectrum peaks at about 15 GeV, with ~ 90% of the spectrum below 100 GeV. Experimental details of the scanning, measurement and reconstruction procedure will be given elsewhere.<sup>(2a)</sup> For the present analysis muons have been selected by a transverse momentum algorithm rather than by the External Muon Identifier (EMI) due to limited geometric acceptance, and in the high intensity running, the excessive hit rate in the EMI.

CC events were required to have the sum of the momenta in the beam direction ( $P_L$ ) from the charged tracks at the production

vertex greater than 7 GeV/c and a reconstructed neutrino energy greater than 10 GeV. For these events the muon was selected as the negatively charged non-interacting track with the highest transverse momentum relative to the total momentum of the other charged tracks. Cuts were also applied to reduce background from CC  $\bar{\nu}$  and NC events<sup>(2b)</sup>. The NC events were selected as those with  $P_{\perp} > 4$  GeV/c where the negative track interacts or where the muon candidate lies on the same side of the beam as the component of the total momentum of the other charged tracks projected into the  $\mu$ - $\nu$  plane.

The reaction (1) was obtained by a 3 constraint kinematic fit. Fits to this reaction with  $\chi^2$  probability  $> 5\%$  were taken in preference to other fits obtained. Ambiguities between the  $\bar{\nu}$  and  $\mu^-$  assignments were resolved by selecting the  $\mu^-$  as described above. The few remaining permutation ambiguities were resolved by selecting the fit with highest probability.

For the other reactions one track had to be identified as a proton either by stopping or by having a significantly better helix fit reconstruction as a proton than a pion<sup>(3)</sup>. Applying this test to protons identified by a 3-C fit to  $\nu p \rightarrow \pi^+ p \mu^-$  we find the criteria select  $.79 \pm .05$  of protons with momentum,  $p_p < 0.5$  GeV/c and  $.55 \pm .05$  for  $0.5 < p_p < 1.0$  GeV/c, and selects a wrong track in  $< 1\%$  of the events. Only identified protons with  $p_p < 1$  GeV/c were accepted.

With an identified proton and (for the CC events) an identified  $\mu^-$ , candidates were selected for reactions 2-5 as follows:

Events with a 3-C fit to any reaction were rejected. Knowing the beam direction, the  $\nu$  energy and the momentum of the missing neutral were calculated by a "0-C fit" for the reactions listed. Events with  $E_d > .02$  GeV were rejected, where  $E_d = E_{out} - m_p - P_L$ , with  $m_p$  the proton mass,  $E_{out}$  and  $P_L$  the sum of the seen outgoing energy and momentum in the beam direction respectively. Events with  $|E_d| < .02$  GeV correspond closely to the 3-C fit sample. Those with  $E_d > .02$  GeV indicate a wrong mass assignment. The samples obtained have a background of events with more than one missing neutral, but these will not give rise to structure in the meson mass spectra studied.

All the invariant mass combinations from the five reactions have been studied in detail. In particular those in which a vector meson may be produced have been studied as a function of  $t' = t - t_{min}$  where  $t$  is the momentum transfer from target proton to final proton. For reactions 2-5, the proton identification procedure restricts  $|t'| \lesssim 0.5$  GeV<sup>2</sup>, the region appropriate for diffractive production. The results and theoretical predictions are summarized in Table I. The backgrounds quoted are estimated from the general shape of the distribution and Monte Carlo calculations. The signal or upper limit results are corrected for scanning and reconstruction losses, proton identification, and where applicable, unobserved decay modes of the resonance. The results have been normalized to the corrected total number of charged current events ( $\sim 3000$ ) and cross sections averaged over the flux distribution have been obtained using measurements from Refs. 4.

The results for each reaction are discussed below:

(1)  $\underline{\nu p \rightarrow \pi^+ \pi^+ \pi^- \mu^-}$  Mass distributions are shown in Fig. 1. A strong  $\Delta^{++}$  signal is observed, and also an enhancement in the region of  $\rho^0$  in the  $\pi^+ \pi^-$  mass distribution. The background in this region is reduced if we plot  $\pi^+ \pi^-$  mass only from those events with  $\pi^+ p$  mass (containing the other  $\pi^+$ ) in the  $\Delta^{++}$  region, suggesting that we are observing the process  $\nu p \rightarrow \rho^0 \Delta^{++} \mu^-$ . The  $\pi^+ \pi^+ \pi^-$  mass distribution is mainly below 1.4 GeV. To study the diffractive production process a selection  $|t'| < 0.5 \text{ GeV}^2$  is made. If in addition one of the  $\pi^+ \pi^-$  mass combinations is required to be in the  $\rho$  region the  $3\pi$  mass distribution is concentrated in the region 0.9 to 1.3 GeV. However, Monte Carlo studies indicate that the  $\Delta^{++}$  produces a strong reflection in this region of the  $\rho^0 \pi^+$  distribution, making it impossible at this level of statistics to identify an  $A_1$  signal. These effects have been taken into account in the upper limit given in Table I.

(2)  $\underline{\nu p \rightarrow \pi^+ \pi^0 \mu^-}$  The mass distributions for  $\pi^+ \pi^0$  and  $\pi^+ p$  are shown in Fig. 2. A strong  $\Delta^{++}$  signal is seen in the  $\pi^+ p$  mass distribution. In the  $\pi^+ \pi^0$  distribution an enhancement is observed in the  $\rho$  region. If events with  $Q^2 > 2 \text{ GeV}^2$  are removed the background is reduced. If in addition events with  $\pi^+ p$  in the  $\Delta^{++}$  are removed the low mass background is much reduced revealing a clear  $\rho^+$  signal of 13 events above an estimated background of 3 events.<sup>(8)</sup>

(3)  $\underline{\nu p \rightarrow \pi^+ \pi^+ \pi^- \pi^0 \mu^-}$  Selected mass distributions are shown in Fig. 3. The only structure observed is a clear  $\Delta^{++}$  signal. The  $\pi^+ \pi^- \pi^0$  mass resolution in the region of  $\omega$  is  $\sim 30 \text{ MeV}$

but there is no  $\omega$  signal, nor indication of  $B^+$  decaying to  $\pi^+\omega$ . The accumulation of events in the region 1.70 to 1.90 GeV in the  $\pi^+\pi^+\pi^-\pi^0$  distribution is consistent with the distribution obtained by a Monte Carlo model, assuming a transverse momentum limited phase space distribution, with the observed fraction of  $\Delta^{++}$  production and restricted  $t'$  distribution.

(4)  $\underline{vp \rightarrow \pi^+\pi^-\nu}$  and (5)  $\underline{vp \rightarrow K^+K^-\nu}$ . The events selected for these channels include a large background from hadronic and CC events. However, there is no indication of structure in the  $\pi^+\pi^-$  or  $K^+K^-$  mass distribution.

The observation of the process  $\nu p \rightarrow \mu^- \rho^+ p$  provides the first test of Conserved Vector Current hypotheses (CVC) away from  $Q^2 = 0$ . Our results are in good agreement with the predictions of Chen et al. (1a). However, Bartl et al (1b) and Gaillard et al (1d), using the simple Vector Dominance Model  $Q^2$  dependence, would predict  $\sim 40\%$  of  $\rho^+$  production with  $Q^2 > 2 \text{ GeV}^2$ , whereas we observe that the  $\rho$  signal has  $Q^2 < 2 \text{ GeV}^2$ . Further information on the correct  $Q^2$  dependence can be obtained by examining the  $y$  distribution of these events, which is all below  $y=0.4$  and peaks at  $y \sim 0.15$ . Within limited statistics the energy distribution of the  $\rho^+$  events is consistent with an energy independent cross section between 10 and 100 GeV.

The  $A_1^+$  is supposed to play the same role for the axial vector current as the  $\rho^+$  does for the vector current, hence the observation of  $\nu p \rightarrow \mu^- A_1^+ p$  would provide a crucial test. The upper limit obtained for this process is well above the predictions

of Ref. 1a, but a factor of 5 below those of Ref. 1d. For NC reactions the upper limits presented are well above the predicted rates.

Production of the  $B^+$  meson has been suggested as a test for second class weak currents<sup>(5)</sup>. To interpret our result as a limit on second class currents it is necessary to have a value for  $f_B$ , the coupling constant of the B to a second class current. In Ref. 5 a model for  $f_B$  was given, introducing a factor K multiplying the second class current term with K=1 corresponding to universality with first class currents. The authors use K=1, consistent with the nuclear results available at that time, to obtain the predicted cross sections given in Table I. Thus, within the assumptions of the model<sup>(5,1a)</sup> our results give a 90% confidence level upper limit for the parameter  $K < 0.3$ . The latest nuclear experiments<sup>(6)</sup> expressed in terms of this parameter give a limit  $K < 0.1$ , thus our result confirms the nuclear results using completely different model assumptions.

To summarize, we have observed diffractive production of  $\rho^+$  as predicted by models applying CVC to electro production results<sup>(1a)</sup>. We are unable to isolate an  $A_1^+$  signal due to reflection effects of  $\Delta^{++}$ , but the limits we obtain are consistent with predictions<sup>(1a,1b)</sup>. From the non-observation of  $B^+$  production we obtain a limit on the strength of second class weak currents, within the assumptions of the model of Ref. 5,1(a), comparable with the limits from latest nuclear experiments<sup>(6)</sup>.

References and Footnotes

- 1(a). M.S. Chen, F.S. Henyey, G.L. Kane, Nucl. Phys. B118 (1977) 345.
- (b). A. Bartl, H. Fraas, W. Majeratto, Phys. Rev. D16 (1977) 2124.
- (c). M.K. Gaillard and C.A. Piketty,  
Orsay Preprint LPTENS 77/5  
March 1977.
- (d). M.K. Gaillard, S.A. Jackson, D.V. Nanopoulos, Nucl. Phys. B102 (1976) 326, and Erratum Nucl. Phys. B112 (1976) 545.
- (e). C.A. Piketty and L. Stodolsky, Nucl. Phys. B15 (1970) 571
- (f). B.P. Roe, Phys. Rev. Lett. 21 (1968) 1666; 23 (1969) 692.
- 2.(a) FNAL, U. of Hawaii, LBL, U. of Michigan, Experimental Study of Hadrons Produced in High Energy Neutrino-Proton Interactions(to be submitted).
- (b) Cuts  $y < 0.9$  and cut on R as in Appendix B. Ref. 2a.
3. A non-stopping track was taken to be a proton if  $R > 1.45$  (1.30) for event processed through HYDRA (TVGP) geometry, where R is the ratio of the pion to proton mass dependent helix fit residuals.
4. B.C. Barish et al., Phys. Rev. Lett 39 (1977) 1595; and D.C. Cundy, Invited talk at APS DPF meeting Argonne National Laboratory October 1977.  $\sigma_{vp}$  was obtained with  $\sigma_n/\sigma_p = 1.93 \pm 0.05$  as calculated using quark distribution of Field and Feynman, Phys. Rev. D15 (1977) 2590.
5. M.S. Chen, F.S. Henyey and G.L. Kane, Nuc. Phys. B114 (1976) 147.

6. See for example review by F. Calaprice, Proceedings of 4th International Conference on Hyperfine Interactions, New Jersey, June 1977. The parameter  $\mathcal{E}_{II}/\mathcal{E}_A \approx -7.7K$  (See Ref. 5)
7. The theoretical predictions have been evaluated by averaging over the neutrino energy spectrum from this experiment. A factor of two has been included in the prediction from 1(a) to correct for an error in that paper. The two predictions for each case from Ref. 1(a) are from their models (III) and (I) , the two extreme cases.
8. The CC muon selection for all events in the  $\rho$  signal has been confirmed by the EMI information.

Reaction	Resonance	Number of events (raw data)	Estimated Background	Signal or 90% confidence upper-limit fraction of total c.c.%		Theoretical Predictions		
				(10 <sup>-40</sup> cm <sup>2</sup> )	(10 <sup>-40</sup> cm <sup>2</sup> )	Ref 1a	Ref 1b	Ref 1d
(1) $\nu\pi^+\pi^+\pi^-\pi^-\pi^0\pi^0$ (75 events) (all t')	$\Delta^{++}\pi^+\pi^0$	64	16	2.1±.4	25±4			
	$\rho^+\pi^+\pi^-\pi^0$	52	38	.6±.3	7±3			
	$\Delta^{++}\pi^0$	25	13	.5±.2	6±3			
	$A_1\pi^+\pi^0$	13	8	<.9	<11	2.5-3.5	15	55
	$\rho^+\pi^+\pi^0$	16	3	.7±.2	8±3	5-9	14	24
(2) $\nu\pi^+\pi^+\pi^-\pi^0\pi^0$ (82 events)	$\omega\pi^+\pi^-\pi^0$	6	6	<.2	<3			
(3) $\nu\pi^+\pi^+\pi^-\pi^0\pi^0\pi^0$ (88 events)	$B^+\pi^+\omega$	2	2	<.2	<2	22-26	-	-
(4) $\nu\pi^+\pi^+\pi^-\pi^0\pi^0$ (33 events)	$\rho^0\pi^+\pi^-\pi^0$	8	6	<.8	<9	~0.8	0.5	.7
	(5) $\nu\pi^+\pi^+\pi^-\pi^0\pi^0$ (13 events)	$\phi\pi^+\pi^-\pi^0$	0	0	<.7	<7	-	0.2

Table I. Summary of results and theoretical predictions.

Mass ranges were taken as  $\Delta$ , 1.08-1.4;  $\rho$ , .65-.9;  $\omega$ , .73-.83;  $B$ , 1.1-1.35;  $\phi$ , .99-1.1;  $A_1$ , 0.9-1.3 GeV. Results are for all  $Q^2$ , but the selection  $Q^2 < 2$  GeV<sup>2</sup> makes no significant reduction in the signal or limits. Prediction from Ref. 1b is for  $Q^2 < 2$  GeV<sup>2</sup>.

FIGURE CAPTIONS

1. Mass distributions of (a)  $\pi^+p$ , (b)  $\pi^+\pi^-$ , and (c)  $\pi^+\pi^+\pi^-$  from reaction (1),  $\nu p \rightarrow \pi^+\pi^+\pi^-\mu^-$ . The hatched area in (a) [(b)] is from events with the other  $\pi^+$  in the  $\rho, [\Delta^{++}]$  region. The hatched area in (c) is from events at low  $t'$  ( $|t'| < 0.5 \text{ GeV}^2$ ), and the cross hatched area is with the additional requirement that one of the  $\pi^+\pi^-$  combinations be in the  $\rho$  region. The solid area is with the additional condition,  $Q^2 < 2 \text{ GeV}^2$ .
2. Mass distributions of (a)  $\pi^+\pi^0$  and (b)  $\pi^+p$  from reaction (2),  $\nu p \rightarrow \pi^+\pi^0\mu^-$ . The hatched area in (a) is events with  $Q^2 < 2 \text{ GeV}^2$ , and the solid area with  $Q^2 < 2 \text{ GeV}^2$  and events with  $\pi^+p$  mass in  $\Delta^{++}$  removed.
3. Mass distributions of (a)  $\pi^+\pi^-\pi^0$ , (b)  $\pi^+\pi^+\pi^-$ , (c)  $\pi^+\pi^+\pi^-\pi^0$  and (d)  $\pi^+p$  from reaction (3),  $\nu p \rightarrow \pi^+\pi^+\pi^-\pi^0\mu^-$ . The hatched area in the plots is for events with  $Q^2 < 2 \text{ GeV}^2$ . The solid area in (c) is with the additional requirement that  $n(\pi^+\pi^+\pi^0)$  be in the  $\omega$  region.

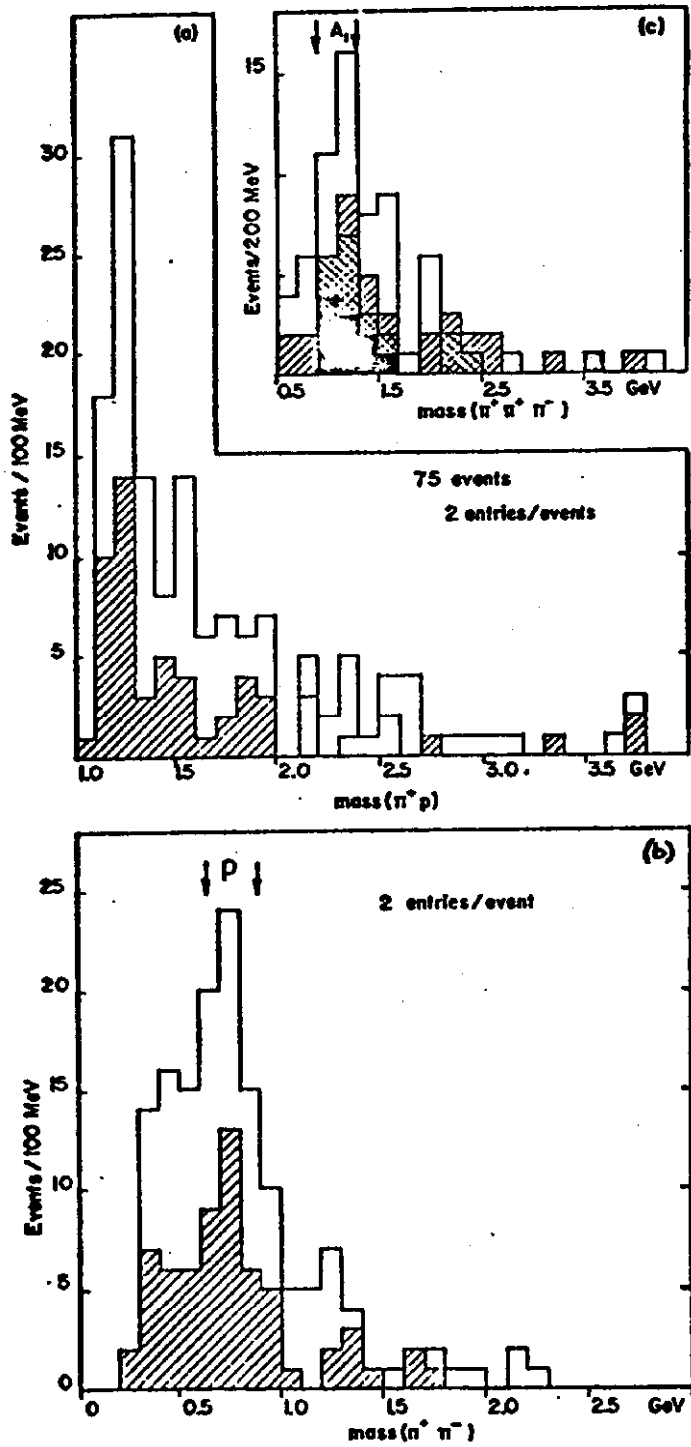


Fig. 1

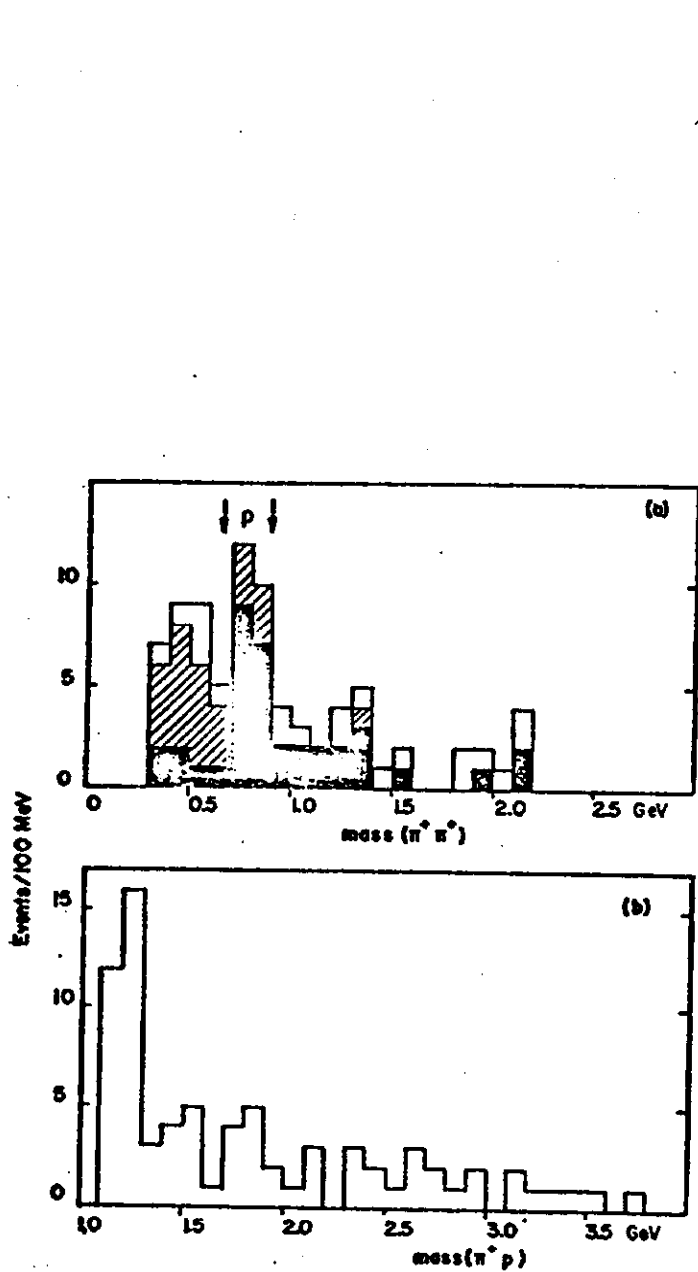


Fig. 2

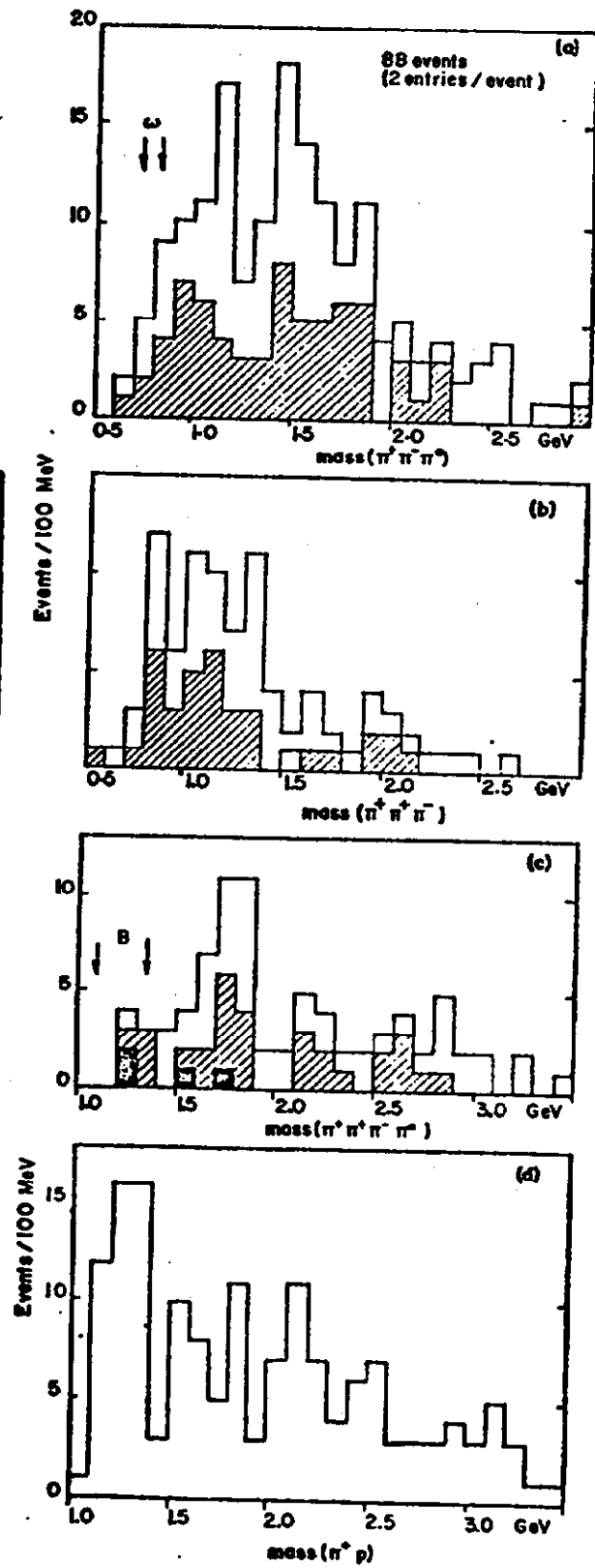


Fig. 3